https://doi.org/10.1016/j.compositesa.2018.03.020

Effect of characteristics of assembly unit of CNT/NCB composite fillers on properties of smart cement-based materials

Liqing Zhang [1], Siqi Ding[2], Linwei Li[1], Sufen Dong[1], Danna Wang[1], Xun Yu[3,4], Baoguo Han [1, *]

[1] School of Civil Engineering, Dalian University of Technology, Dalian 116024, China
[2]Department of Civil and Environmental Engineering, The Hong Kong Polytechnic University, Hung Hom, Kowloon, Hong Kong
[3]Department of Mechanical Engineering, New York Institute of Technology, New York, NY 11568, USA
[4]School of Mechanical Engineering, Wuhan University of Science and Technology, Wuhan, 430081, China
* Corresponding author: hithanbaoguo@163.com, hanbaoguo@dlut.edu.cn

Abstract: A type of electrostatic self-assembly CNT/NCB composite fillers with high CNT aspect ratio and large NCB size was incorporated into cement-based materials to develop smart cement-based composites. The mechanical, electrical and piezoresistive properties of the cement-based materials with CNT/NCB composite fillers are investigated. Percolation equation is used to describe electrically conductive property. Electrochemical impedance spectroscopy and equivalent circuits are used to explore the conductive and mechanical mechanism. The research results show that cement-based materials with CNT/NCB composite fillers at low content present acceptable mechanical property, high conductive property and stable and sensitive piezoresistive property. The fractional change of electrical resistivity, stress and strain sensitivity of cement-based materials with 1.41 vol. % CNT/NCB composite fillers can reach 13.4 %, 3.12 %/MPa and 521, respectively. It is concluded that high CNT aspect ratio and large NCB size in CNT/NCB composite fillers are beneficial for improving the properties of smart cement-based composites.

Key words: A. Multifunctional composites; A. Smart materials; B. Electrical properties; E. Assembly

1 Introduction

With the continuous development of social economy, a variety of large and complex civil infrastructures have emerged as long-term accommodation platform and space for

residents. However, due to the aggressive service environments such as fatigue load, earthquake, wind, corrosive liquids and gases, the security of civil infrastructures is under threat. Thus, the monitoring of real-time condition and performance, i.e. structural health monitoring (SHM), is very important. SHM is normally performed by measuring the critical responses of a structure's critical zone with various sensors. Based on the collected data, the health of the structure can be tracked and evaluated to make decisions on structure maintenance. With prompt maintaining work, the safety and reliability of civil infrastructures can be enhanced to ensure their serviceability and sustainability [1]. Without doubt, sensor technology plays an important role in SHM. There are some traditional strain sensors widely used in SHM, such as electrical resistance strain gauges, optical fiber [2-4], shape memory alloy [5, 6], and piezo-electric (PZT) ceramics [7-9]. Apart from traditional strain gauges, Chung firstly developed a new type of strain senor by adding carbon fiber into cement-based materials, which has high sensitivity, good property and natural compatibility [10]. This type of cement-based strain senor is also named intrinsic self-sensing concrete (ISSC), which is fabricated by incorporating functional fillers into conventional cement-based materials to increase its ability to sense the strain, cracks or damage inside while maintaining or even improving its mechanical properties and durability [11-14]. Chung's team also made a series of systematic research about cement-based sensors with carbon fiber which have been used for traffic monitoring, weighing in motion [15, 16]. Mao et al. studied the resistance of carbon fiber reinforced cement-based materials under different pressures [17]. Sun et al. fabricated carbon fiber reinforced cement-based materials to monitor thermal property [18]. Reza et al. explored the change of electrical resistance in compact tension of carbon fiber reinforced cement-based materials [19]. Han et al. explored the piezoresistivity of cement-based materials with

carbon fiber and nano carbon black (NCB) under single compressive loading and repeated compressive loads at different loading amplitudes, and found that it is reversible and stable within the elastic regime [20]. After that, Han et al. studied the self-sensing cement-based materials with NCB [21], cement-based materials with nickel powder [22], cement-based materials with CNT [23]. Long et al. fabricated cement-based materials with NCB and explored their piezoresistive property [24]. Li et al. introduced NCB into cement-based materials and found it owns self-sensing capability [25]. Yu et al. investigated piezoresistive property of carbon nanotube (CNT) reinforced cement-based materials and found that the electrical resistance of the composite changed synchronously with the compressive stress levels [26]. Materazzi et al. explored the applicability of CNT cement-based sensors for measuring dynamically varying strain in cement-based structures [27]. Ubertini et al. proved the feasibility of using CNT cement-based sensor to vibration monitoring of reinforced cement-based structures [28]. You et al. [29] and Samsal et al. [30] also fabricated cement-based sensors with CNT. García-Macías et al. built a micromechanics modeling of the uniaxial strain-sensing property of cement-based materials with CNT, which is helpful for SHM applications [31].

It can be found that the functional fillers, such as carbon fiber (CF) [18, 19, 32-36], steel fiber [37], nano graphite platelets [38], spiky spherical nickel powders [22], CNF [39, 40], CNT [29, 41], nano carbon black (NCB) [42, 43], in ISSC shift from microscale to nanoscale. ISSC with nanoscale fillers has many advantages over it with microscale fillers, such as high sensitivity and low content. In addition, the type of functional fillers used in ISSC changing from single to hybrid is another development direction. This can take advantage of different types of fillers thus achieving positive summing effect [44]. Therefore, CNT/NCB composite fillers are promising fillers for

fabricating self-sensing cement-based materials. The cement-based materials with high strain sensibility have been successfully developed by using CNT/NCB composite fillers in reference [44]. Characteristics of assembly unit of CNT/NCB composite fillers, such as CNT diameter, CNT length and NCB size would strongly affect their electrically conductive property and dispersity. CNT in assembly unit with high aspect ratio can easily form conductive network in cement-based materials. As for NCB in assembly unit with big diameter can not only participate in short-range conductive, but also improve dispersion of CNT. However, to the best of our knowledge, the effect of characteristics of assembly unit of CNT/NCB composite fillers on the properties of cement-based materials has not been investigated.

Therefore, self-assembly CNT/NCB composite fillers with high CNT aspect ratio and large NCB size are incorporated into cement-based materials in this paper. The flexural and compressive strength, direct current (DC) and alternating current (AC) electrical resistivity, piezoresistive properties in elastic regime and under ultimate load of cement-based materials with CNT/NCB composite fillers have been studied. In addition, percolation equation is used to describe DC and AC electrically conductive property. Electrochemical impedance spectroscopy and equivalent circuits are used to explore the conductive and mechanical mechanism.

2 Experimental methods

2.1. Raw materials and specimen preparation

2.1.1 Raw materials

The cement-based materials in this paper are fabricated by cement, silica fume, water, sand, polycarboxylate superplasticizer and CNT/ NCB composite fillers. 42.5R ordinary Portland cement (Dalian Onoda Cement Co. Ltd., China) and silica fume (920D type, Shanghai Tian Kai Silicon Fume Co. Ltd., China) are used as binder

materials. Standard sand is provided by Xiamen Ai Si Ou Standard Sand Co. Ltd., China. Polycarboxylate superplasticizer (3310E, Dalian Sika) has a solid content of 45%. CNT/NCB composite fillers (Chengdu institute of organic chemistry Co., Ltd.) are shown in Fig. 1. Their properties are listed in Table 1, which are different from the CNT/NCB composite fillers in reference [44]. It should be noted that the CNT/NCB composite fillers used in this paper include CNT with small diameter and large length.

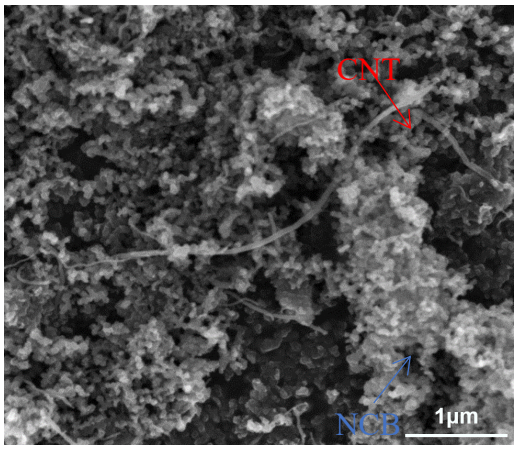

Fig.1 SEM photograph of CNT/NCB composite fillers

Table 1 Main properties of CNT/NCB composite fillers

Ingredient	Composition (CNT:NCB)	Resistivity (Ω.cm)	Specific surface area (m^2/g)	Out diameter of CNT(nm)	Specific surface area of NCB(m^2/g)
CNT/NCB	40:60	＜0.01	540~560	10-30	934

2.2.2 Specimen preparation

The mixing proportions of cement-based materials with CNT/NCB composite fillers are shown in Table 2.

The specimen fabrication process is described as follows. Firstly, silica fume and CNT/NCB composite fillers were put into the stirring pot and dry mixed by mortar stirrer at a low speed (140±5r/min) for 30s. Secondly, water and the polycarboxylate superplasticizer were added into the pot and stirred for a 30s low-speed stir again.

Thirdly, half of the pre-weighed cement was poured in the pot and stirred at a slow speed for 60s and at a high speed (285±10 r/min) for 30s. Fourthly, the other half cement was put in and followed by a slow 60s stir and then a quick 30s stir. Standard sand was added for a slow 60s stir and then a quick 30s stir. At last, a slow 60s stir and then a quick 30s stir were required.

The well-stirred fresh mixtures were put into the corresponding oiled molds. The sizes of molds were 40mm×40mm×160mm for flexural strength test, 40mm×40mm×80mm without electrodes for compressive strength test, and 40mm×40mm×80mm with electrodes for piezoresistive test (as show in Fig. 2). Three specimens were prepared for each test. All specimens were demolded after 24 hours in standard curing box (90% RH, 20±1°C). Then they were cured in water with a temperature of 20±1°C for 27d to complete 28d of curing.

Table 2 Mixing proportions of all specimens

Serial number	Binder	Fillers (vol. %)	Water to binder ratio	Water reducer (wt. %)	Sand to binder ratio
S0	1	0.00	0.42	0.0	1.5
S1	1	0.39	0.42	0.0	1.5
S2	1	0.77	0.42	1.4	1.5
S3	1	1.41	0.48	3.7	1.5
S4	1	2.14	0.72	5.4	1.5

Note: (1) Binder is composed of cement and silica fume. Here makes the mass of binder a unity 1 and mass of silica fume accounts for 10% of binder; (2) Volume percent of CNT/NCB composite fillers is relative to the whole material; (3) The mass percentage of water reducer is based on that of binder.

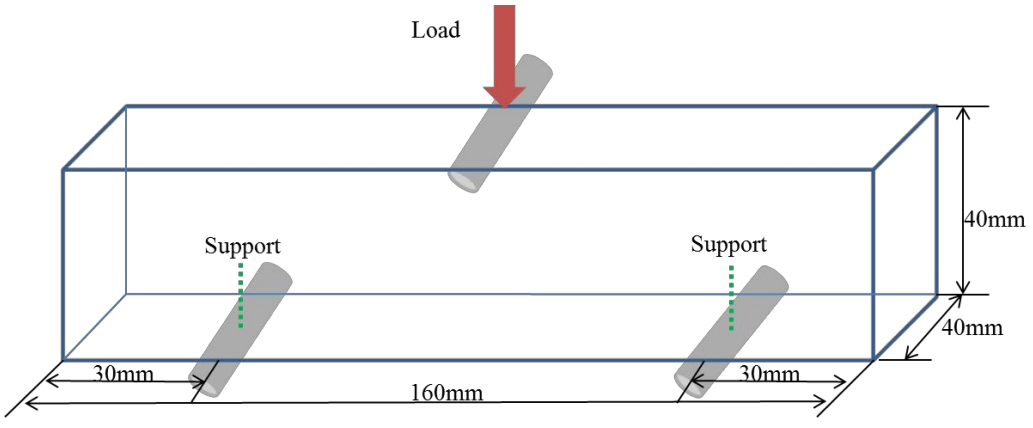

(a) Flexural strength test

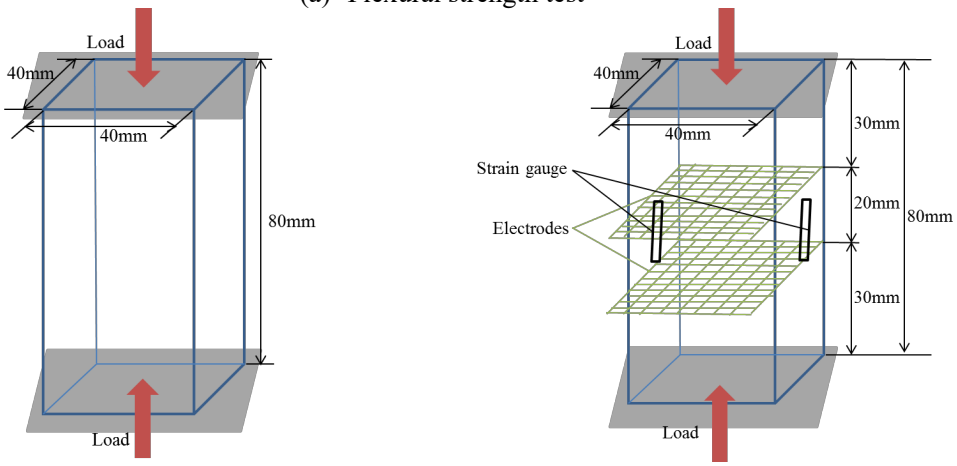

(b) Compressive strength test (c) Piezoresistive test

Fig. 2 Sketch of the specimens for (a) flexural strength test, (b) compressive strength test and (c) piezoresistive test

2.2. Measurement

2.2.1 Mechanical measurement

The flexural strength of hardened specimens after 28d curing was measured by a mortar folding meter DKZ-5000 (Wuxi Jian Yi Instrument Mechanical Co. Ltd., China). The flexural loading speed is 50±10N/s. The compressive strength of hardened specimens after 28d curing was measured by a universal electronic testing machine WDW-200E (Jinan Time Assay Machine Co. Ltd., China). The compressive loading speed is 0.4mm/min.

2.2.2 Electrical measurement

At the curing age of 3d, 7d, 14d, 21d, and 28d, specimens were taken from the water and wiped off water then tested electrical resistivity. DC electrical resistivity was measured by two-electrode method, using a Keithley 2100 digital multimeter (Keithley Instruments Inc., USA). The AC electrical resistivity without loading is measured by two-electrode method using an Agilent U1733C Digital Multimeter (Agilent Technologies Inc.). The AC impedance spectroscopy is tested by AC two-electrode

method using an electrochemical workstation (Shanghai Chen Hua Instrument Co., LTD) at 28d curing age.

2.2.3 Piezoresistive measurement

Piezoresistive properties were tested in the elastic regime and during compressive loading to destruction by displacement control and only exerted on the 40mm×40mm×80mm specimens after 28d curing. In elastic phase, the effect of content of fillers, load amplitude and load rate on piezoresistive property were studied. Maximum value of compressive load is 4 MPa and the loading rate is 0.4mm/min for studying the effect of filler content. The load amplitudes of compressive loads are 2 MPa and 4 MPa and the loading rate is 0.4 mm/min for studying the effect of load amplitude. The load amplitude of compressive load is 4MPa and the loading rate is 0.2 mm/min, 0.4 mm/min and 0.8 mm/min for studying the effect of load rate. During compressive loading to destruction, the load rate is 0.4 mm/min.

Compressive loads were applied using WDW-200E. The strain was measured via two strain gauges stuck to the middle of two opposite sides along the longitudinal direction and two strain gauges attached to the middle of the other two sides perpendicular to the longitudinal direction, using DC-204R (Tokyo Sokki Kenkyujo Co. Ltd.). During this process, the DC resistance measurement was carried out in the meantime by using Keithley 2100. The fractional change in electrical resistivity is calculated as $\Delta\rho = 100\% \times (\rho_{min} - \rho_0)/\rho_0$ (where ρ_0 is the resistivity without loading, ρ_{min} is the resistivity under compressive loading). The sampling frequencies for resistance, strain and compressive loading are all 2 Hz.

2.2.4 SEM characterization

SEM NOVA NANOSEM450 (FEI Inc., USA) is used for taking SEM images of the fillers and cement-based materials with CNT/NCB composite fillers.

3 Results and discussion

3.1 Mechanical property

Flexural strength of cement-based materials without and with CNT/NCB composite fillers after curing 28d is shown in Fig. 3. When the water to binder is 0.42, the flexural strength firstly increases then decreases with increasing filler content. When the content of CNT/NCB composite fillers is 0.39 vol. %, the flexural strength is as high as 11.3 MPa which increased 1.8% than that of plain cement-based materials. The increase of flexural strength of S1 is due to crack bridging of CNT and pulling out of CNT (as shown in Fig. 4). With 0.77 vol. % fillers, the flexural strength is 9.7 MPa, which reduces 12.6% compared with plain cement-based materials. When the content of CNT/NCB composites fillers is over 0.77 vol. %, higher water to binder ratios are needed to get workability. High water to binder ratio will reduce the flexural strength. With increasing content of CNT/NCB composite fillers, cement particles will adsorb some fillers. This will affect the hydration of cement, leading to weak strength [45]. The flexural strength of cement-based materials with 2.14 vol. % CNT/NCB composite fillers is the lowest among all the specimens which can also reach 6.2 MPa.

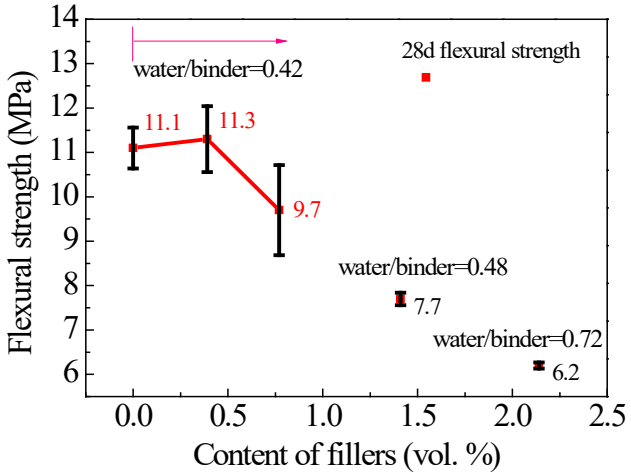

Fig. 3 Flexural strength of cement-based materials with CNT/NCB composite fillers after curing 28d

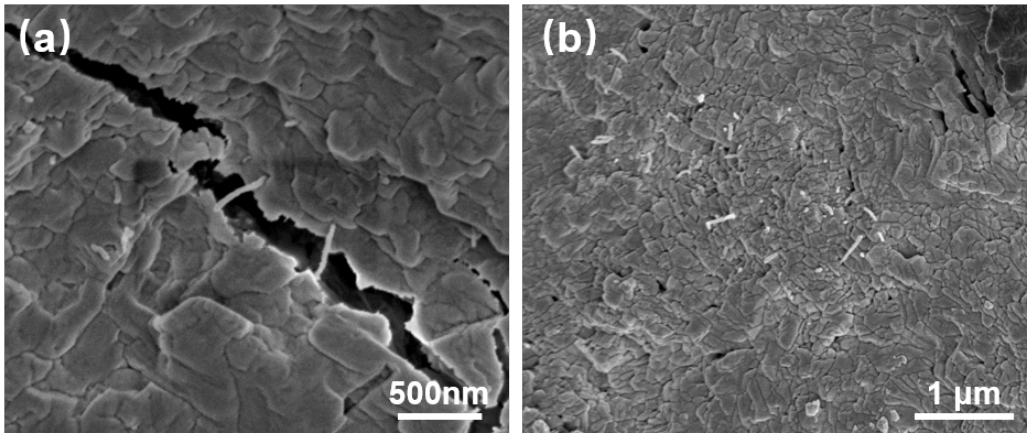

Fig. 4 SEM images of cement-based materials with CNT/NCB composite fillers: (a) crack bridging of CNT, (b) CNT pull out

Compressive strength of cement-based materials with CNT/NCB composite fillers after curing 28d is shown in Fig. 5. With the same water to binder, compressive strength decreases slowly with increasing filler content. When setting compressive strength of S0 as standard, the improvement percent of S1-S2 after curing 28d is -17.5%, -18.3%, respectively. With increasing water to binder ratio, compressive strength decreases. However, the compressive strength of S3 also can reach 30.7 MPa.

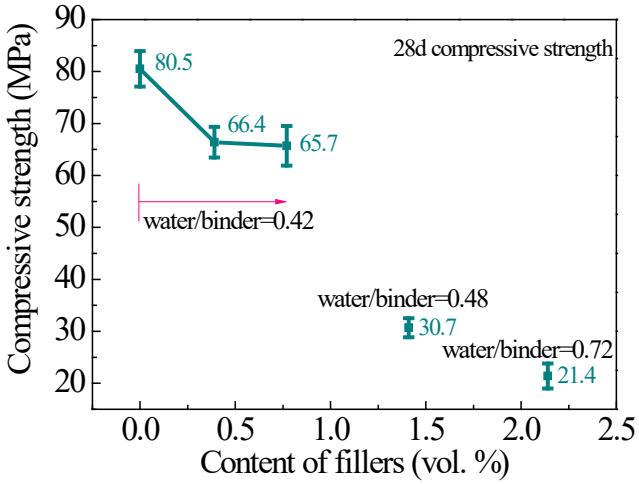

Fig. 5 Compressive strength of cement-based materials with CNT/NCB composite fillers after curing 28d

3.2 Electrical properties

3.2.1 DC electrical resistivity

The DC electrical resistivity of cement-based materials with CNT/NCB composite fillers is shown in Fig. 6. As shown in Fig. 6, the DC resistivity decreases slightly when the filler content is 0.39 vol. % or more than 1.41 vol. %. In addition, the DC resistivity of cement-based materials with 0.39 vol. %-1.41 vol. % fillers decreases sharply. Therefore, the percolation threshold zone is located in 0.39 vol. % -1.41 vol. %.

The conductive network gradually comes into being with increasing content of CNT/NCB composite fillers, as shown in Fig. 7. The main conductive components in cement-based materials with CNT/NCB composite fillers change from electrons and electrolyte ions to electrons with increasing content of fillers. When the content is low, the average center distance between fillers is far. The main electric conduction depends on the transfer of electrolyte ions and electrons. As CNT/NCB composite filler content increases, stable conductive network will be established by the fillers in the matrix. The main electric conduction depends on the tunnel effect of CNT/NCB composite fillers. Continuously increased, some fillers are lapped each other (as shown in Fig. 7(e)). Therefore, the main electric conduction depends on contact conduction.

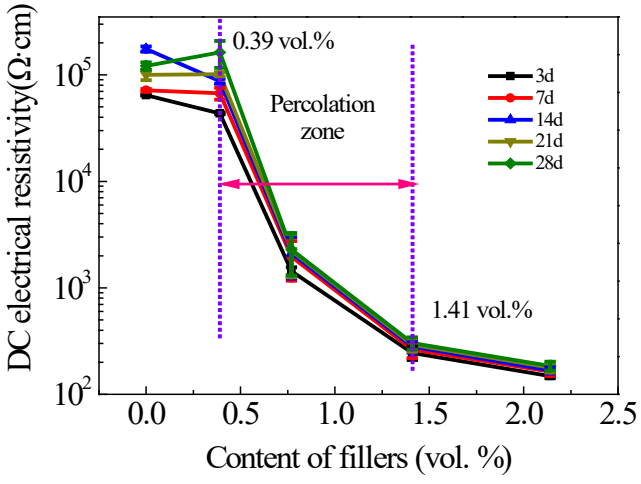

Fig. 6 DC electrical resistivity of cement-based materials with CNT/NCB composite fillers after curing 3d, 7d,14d, 21d and 28d

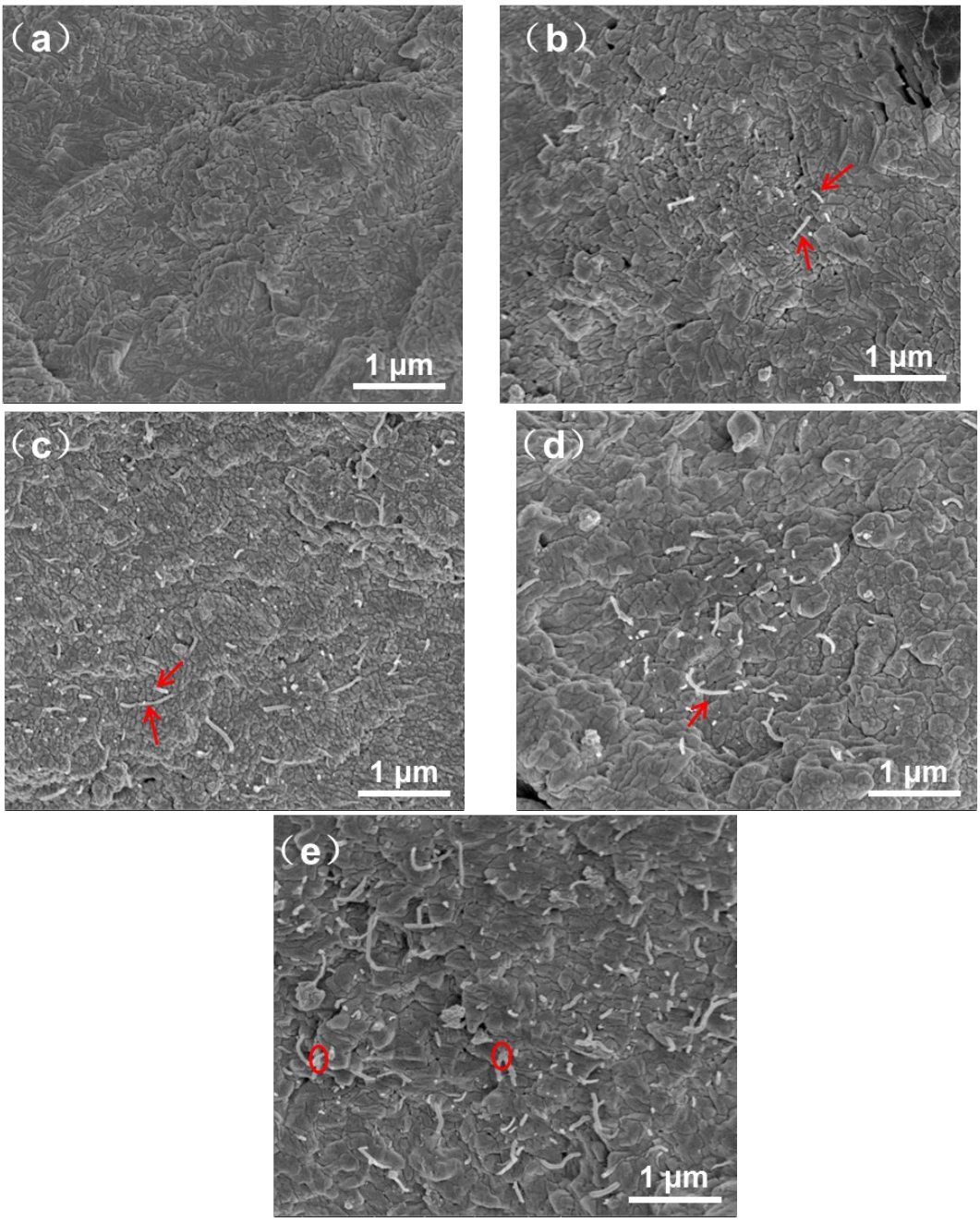

Fig. 7 Conductive network in (a) S0 (0 vol. %)，(b) S1 (0.39 vol. %), (c) S2 (0.77 vol. %), (d) S3 (1.41 vol. %) and (e) S4 (2.14 vol. %) (Arrow: CNT; Circle: overlap CNT)

3.2.2 AC electrical resistivity

AC electrical resistivity of cement-based materials with CNT/NCB composite fillers is shown in Fig. 8. With increasing content of CNT/NCB composite fillers, AC

electrical resistivity decreases. Between 0.39 vol. % and 1.41 vol. %, AC electrical resistivity decreases sharply. Therefore, the percolation threshold zone ranges from 0.39 vol. % to 1.41 vol. %, which agrees with the DC electrical resistivity results. Under the same curing age, AC electrical resistivity of S0-S4 all decreased with increasing frequency (from 100Hz to 100kHz) because a high frequency will weaken the polarization effect. In addition, AC electrical resistivity of cement-based materials with CNT/NCB composite fillers increases with curing ages. It also can be observed that increase rate with aging of AC electrical resistivity of cement-based materials with CNT/NCB composite fillers decreases with increasing content of fillers. The conductive network becomes rich with increasing fillers. Therefore, AC electrical resistivity of cement-based materials with CNT/NCB composite fillers is not sensitive to curing age.

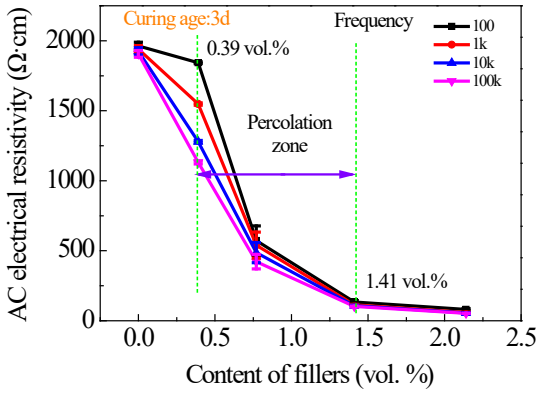

(a) 3d

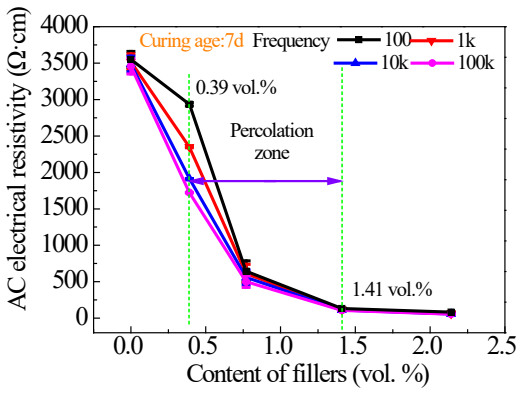

(b) 7d

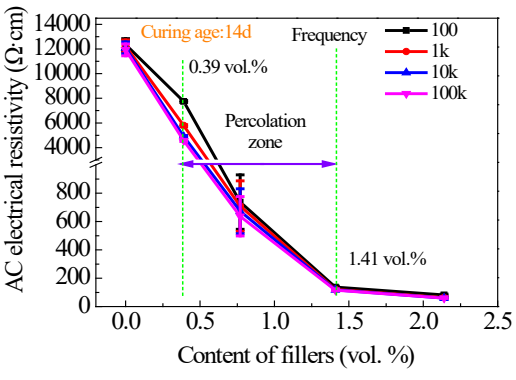

(c) 14d

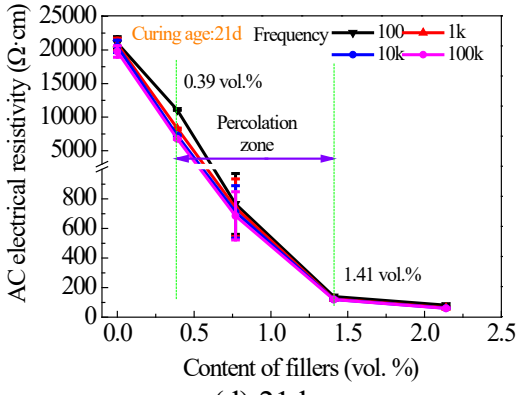

(d) 21d

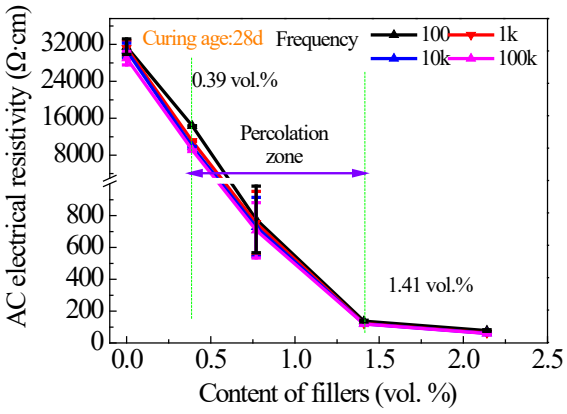

(e) 28d

Fig. 8 AC resistivity of cement-based materials with CNT/NCB composite fillers after curing (a)3d, (b) 7d, (c) 14d, (d) 21d and (e) 28d

Comparison among different researches regarding cement-based materials with CNT or/and NCB is shown in Table 3. As shown in Table 3, cement-based materials with CNT/NCB composite fillers in this paper have a lowest percolation threshold value and highest conductivity. On the one hand, CNT/NCB composite fillers can take advantage of different types of fillers and get positive summing effect compared with single CNT or NCB fillers. On the other hand, CNT/NCB composite fillers in this paper own CNT with high aspect ratio. Based on the middle diameter and length data of CNT and NCB in Table 4, numbers of assembly unit in $1cm^3$ of cement-based materials can be calculated. It can be seen that the volume of assembly unit in reference [44] is about 2.6 times of that in this paper. As show in Table 4, a larger number of fillers exist in cement-based matrix compared with reference [44] when the filler content is constant. As shown in Fig. 9, CNT/NCB composite fillers with CNT owning high aspect ratio and NCB with big size are more easily to form conductive network. Therefore, specimens in this paper can reach lower percolation threshold value with least content fillers.

Table 3 Comparison among different researches regarding cement-based materials with CNT or/and NCB

Filler type	The lowest percolation threshold value	Resistivity (Ω.cm)	Reduction extent (%)	Sources

	(vol. %)			
CNT/NCB composite fillers	1.41	303	99.7	This paper
	1.52	783	99.9	Reference [44]
CNT	1.50	6000	96.5	Reference [12]
	3.00	6512	99.0	Reference [13]
NCB	1.58	300	99.6	Reference [24]
	11.39	100	-	Reference [25]

Table 4 Comparison of two types CNT/NCB composite fillers

Items	Assembly unit in this Paper		Assembly unit in reference [44]	
	CNT	NCB	CNT	NCB
Inner diameter(nm)	7.5	-	10	-
Out diameter(nm)	15	-	50	-
Length (nm)	30000	-	15000	-
Diameter(nm)	-	35	-	23
Volume of every assembly unit (nm^3)	562500		1500000	
Concentration of fillers (vol. %)	1.41		1.41	
Numbers of assembly unit in $1cm^3$ of cement-based materials	25066		940	

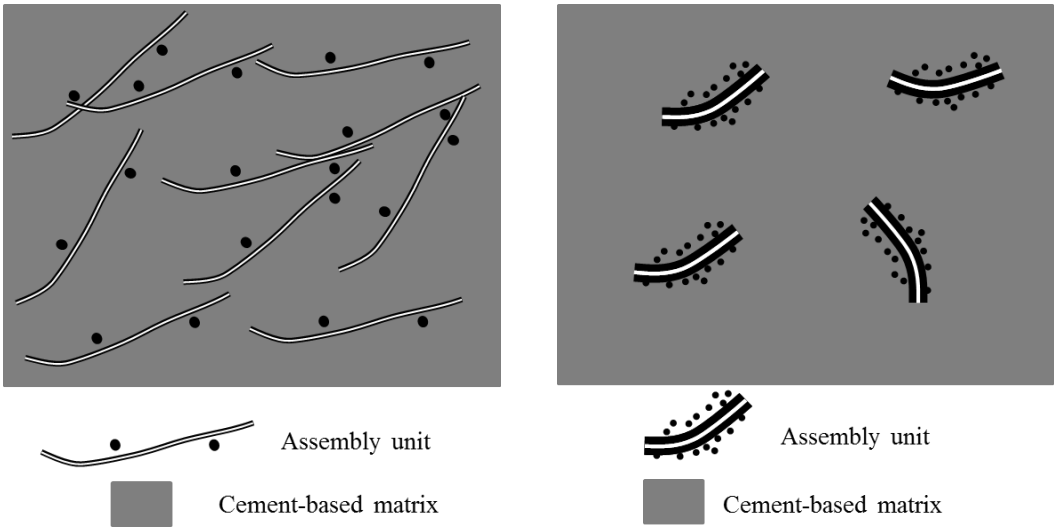

(a) Fillers in this paper owing CNT with small diameter and large length

(b) Fillers in Reference [44] owing CNT with large diameter and small length

Fig. 7 Sketch of cement-based matrix with the same volume content of fillers

3.2.3 Percolation theory

According to percolation theory, the composite conductivity scales with filler volume fraction ϕ as

$\sigma_e \propto (\phi-\phi_{c,e})^{n}_e$

where $\phi_{c,e}$ is the percolation threshold, and n_e is exponent [46]. Conductivity of cement-based materials with CNT/NCB composite fillers tested by DC method, AC method is fitted with this equation, which is shown in Figs. 10-12. The equation fits the DC method data well when $\phi_{c,e}$ is 0.39 vol.% and n_e is between 1.18 to 1.22, as shown in Fig. 10. As for AC method data, the equation can fit the data well when $\phi_{c,e}$ is 0.39 vol.% and n_e is between 1.28 to 1.39, as shown in Fig. 11. The difference of n_e obtained from DC and AC method is due to reduced polarization at high frequency. Therefore, n_e got from DC method is smaller than that obtained from AC method. In addition, it also can be seen from Fig. 12 that n_e reduces with increasing frequency.

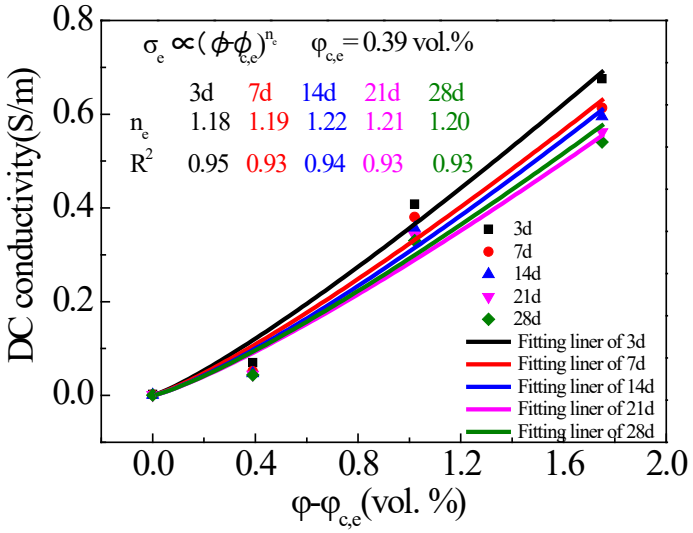

Fig. 10 DC electrical conductivity cement-based materials mortar with CNT/NCB composite fillers as a function of reduced CNT/NCB composite fillers volume fraction, ϕ- $\phi c,e$

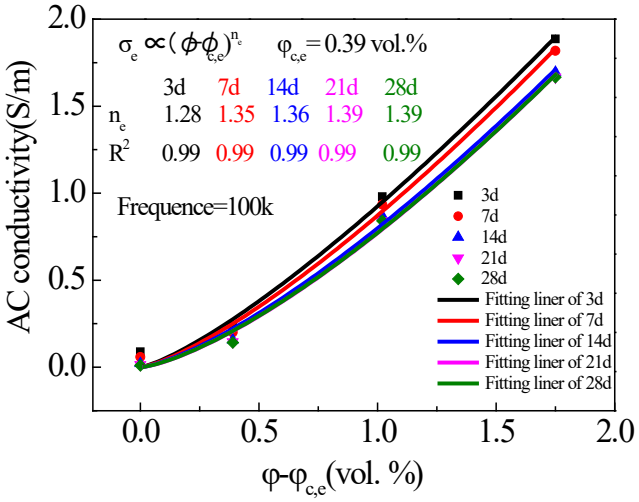

Fig. 11 AC electrical conductivity cement-based materials with CNT/NCB composite fillers as a function of reduced CNT/NCB composite fillers volume fraction, ϕ- $\phi_{c,e}$

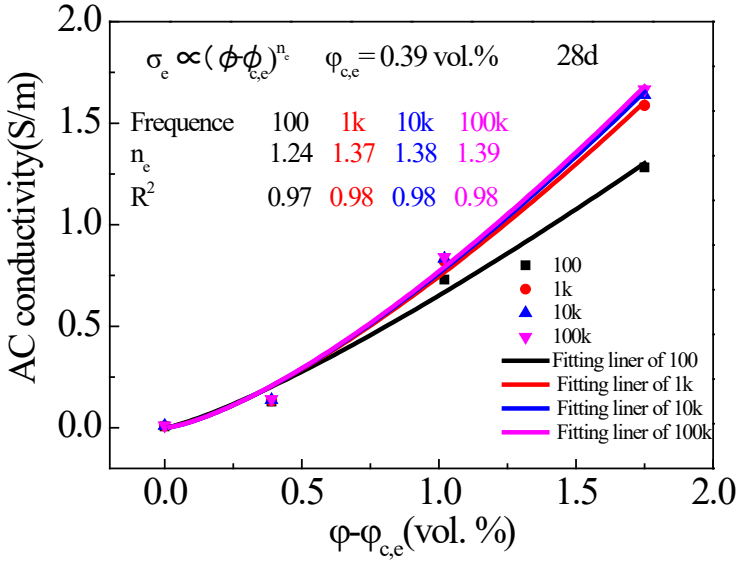

Fig. 12 AC electrical conductivity cement-based materials with CNT/NCB composite fillers as a function of reduced CNT/NCB composite fillers volume fraction, ϕ- $\phi_{c,e}$ after 28d water curing at different frequency

3.2.4 Electrochemical impedance spectroscopy

The EIS and equivalent circuits are used to analyze the mechanisms of conductive and mechanical properties of cement-based materials with CNT/NCB composite fillers [47]. The conductive mechanism is shown in Fig. 13. For plain cement-based materials, in the whole specimen electrochemical impedance spectroscopy (EIS) includes three parts, i.e., the pore solution, the matrix and the electrodes, as shown in Fig. 13(a). Rs is

the resistance of pore solution. Q1 and R1 in parallel represents cement matrix. In addition, Q2 and R2 in parallel represent EIS caused by electrodes and wires. Therefore, the equivalent circuit, i.e. Rs(Q1R1)(Q2R2), can be used to describe the EIS of plain cement-based materials. For the cement-based materials with fillers, there are the pore solution, the cement matrix, the conductive fillers and cement matrix, and the electrodes, as shown in Fig. 13(b). Q3 and R3 in parallel represent the conductive fillers and cement matrix. Then, the equivalent circuit is Rs(Q1R1) (Q2R2)(Q3R3).The EIS measured results and calculated results using Zsimpwin according equivalents of S0-S4 can be drawn in Nyquist plot and shown in Fig. 14. In Fig. 14, Zr and Zi are the real and imaginary components, respectively, and the frequency decreases from left to right. The Chi-squared is less than or equal to $4.05 \times .0^{-4}$. This suggested that the selected equivalent circuits are reasonable for describing the conductive nets and structures in S0-S4.

Topological structures of EIS of S0-S4firstly change and then keep similar, which indicates that the structures and numbers of conductive paths change with increasing filler content. The linear part of EIS of S1 (with 0.39 vol.% fillers), controlled by charge diffusion, disappears. This means that the CNT/NCB composite fillers have played an important role in the conductive paths. The topological structures of EIS of S2-S4 are similar. It illustrated that the percolation network has formed when the filler content is 0.77 vol. %. This is in accordance with the test results of electrical resistivity.

In addition, the electrical resistance of pore solution (*Rs*) in cement-based can be calculated using Zsimpwin and is shown in Table 5. With increasing filler content, the values of *Rs* decrease, i.e., the porosity of the cement-based materials increases, which are in accordance with the test results of compressive strength.

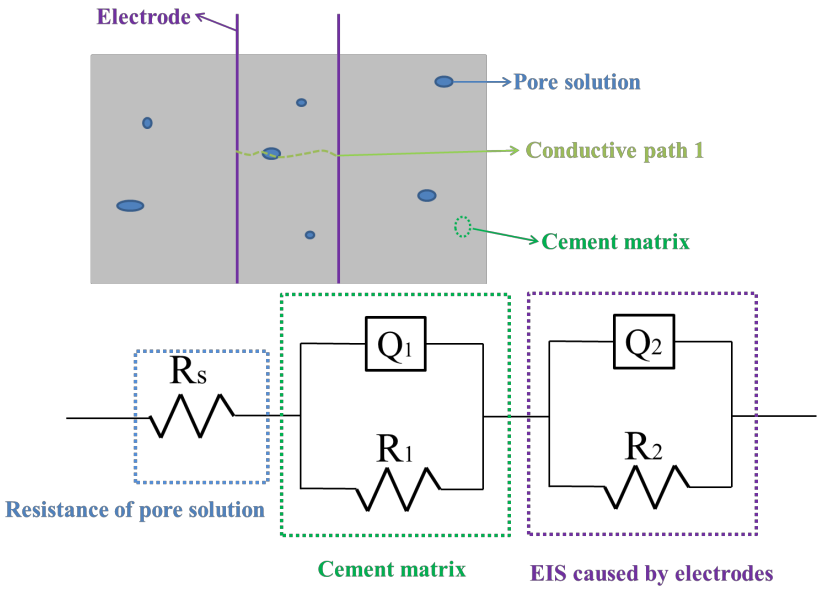

(a) Plain cement-based materials

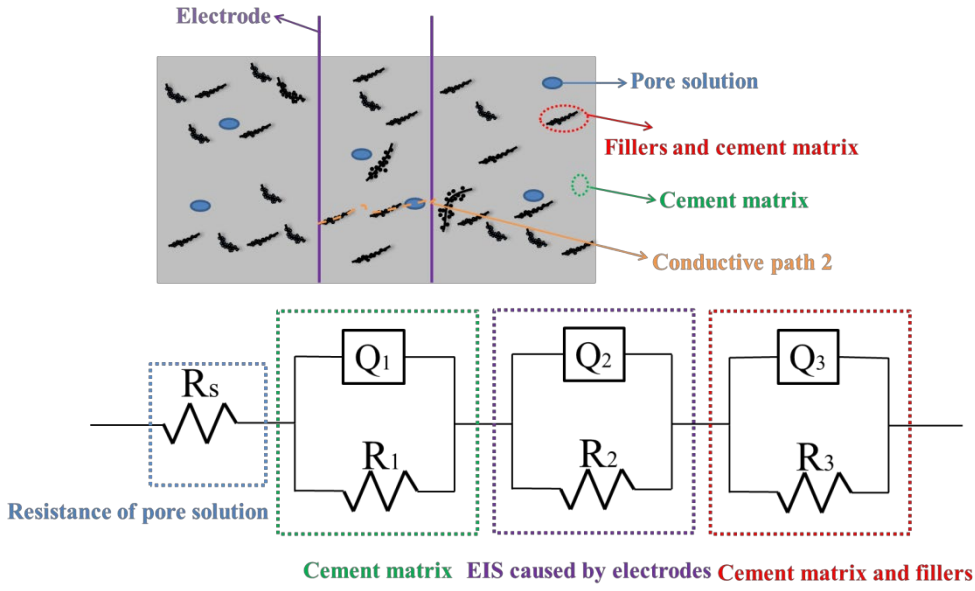

(b) Cement-based materials with CNT/NCB composite fillers

Fig. 13 The equivalent circuits of cement-based materials with different contents of CNT/NCB composite fillers: (a) plain cement-based materials; (b) cement-based materials with CNT/NCB composite fillers

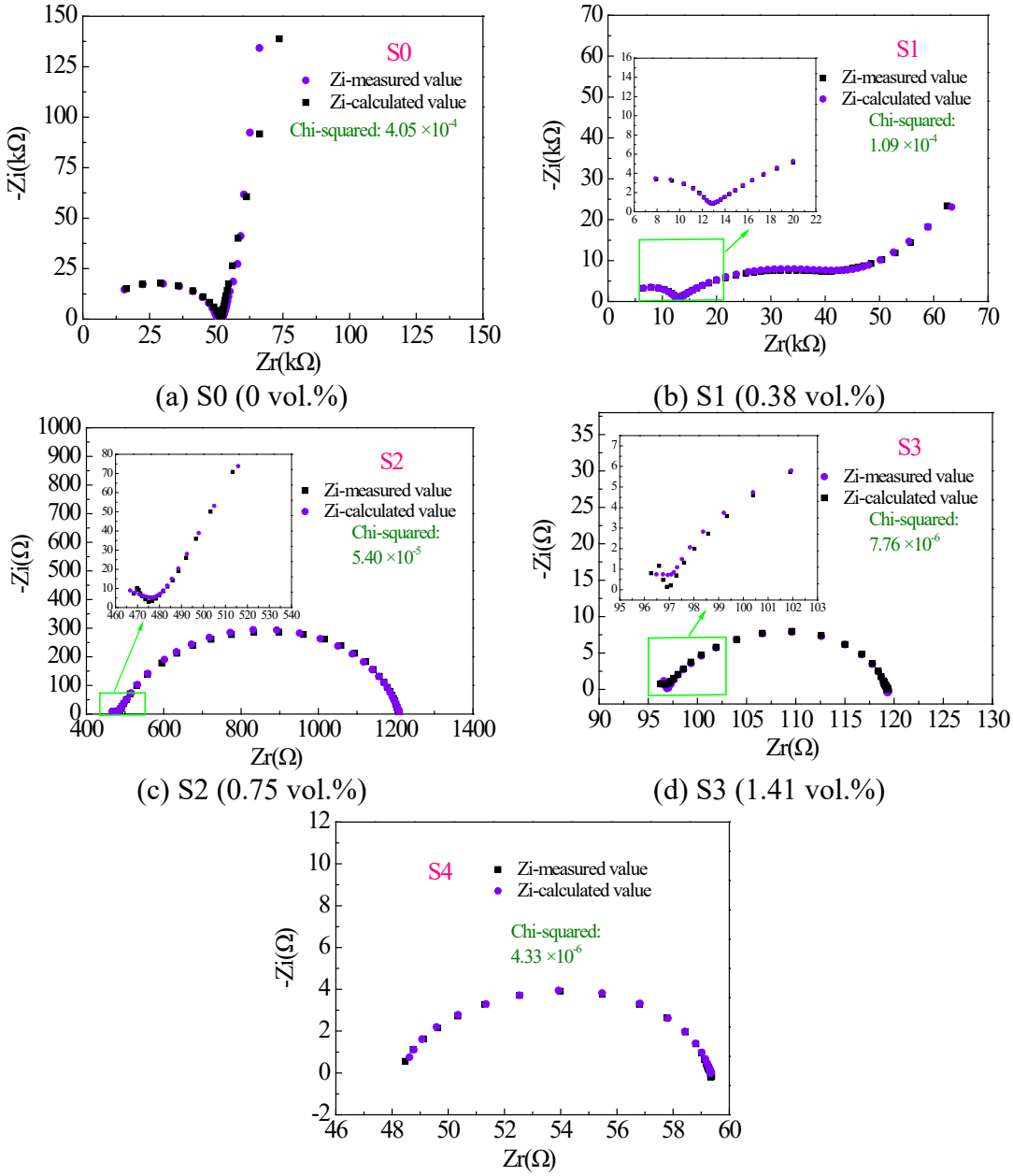

(a) S0 (0 vol.%) (b) S1 (0.38 vol.%)

(c) S2 (0.75 vol.%) (d) S3 (1.41 vol.%)

(e) S4 (2.14 vol.%)

Fig. 14 EIS curves of cement-based materials with different content of CNT/NCB composite fillers: (a) S0, (b) S1, (c) S2, (d) S3, (e) S4

Table 5 Elements parameters of the equivalent circuit models in Fig. 12

Specimen	S0	S1	S2	S3	S4
Rs (Ω)	3660	3526	323	96	48

3.3 Piezoresistive property

3.3.1 Piezoresistive property in elastic regime

(1) Effect of filler content on piezoresistive property

Compressive stress/strain and fractional change in electrical resistivity of S0-S4 under cyclic compressive loading with stress amplitude of 4 MPa are shown in Fig. 15, which is tested after 28d water curing. The overall trend of S0-S4 is all the same. The fractional change in electrical resistivity decreases as the compressive stress/strain increases, and it increases as stress/strain decreases. That means all specimens have piezoresistive property. The fractional change in electrical resistivity of S0-S1 firstly increases then decreases with increasing content of CNT/NCB composites fillers (as shown in Fig. 15 (m)). From Fig. 15, S3 has the maximum fractional change in electrical resistivity among all specimens and S4 followed. Maximum fractional change in electrical resistivity of S0 is 1.1%. It has a slight increase trend due to the polarization, while the phenomenon is not obvious. Maximum fractional change in electrical resistivity of S1-S4 is with absolute value of 1.8%, 1.4%, 13.4% and 12.9% corresponding to 178με, 182με, 257με, and 333με of strain, respectively. Therefore, lower content of fillers has little contribute to piezoresistivite property. When the filler content is up to 1.41 vol. %, it will play a significant role in piezoresistive property.

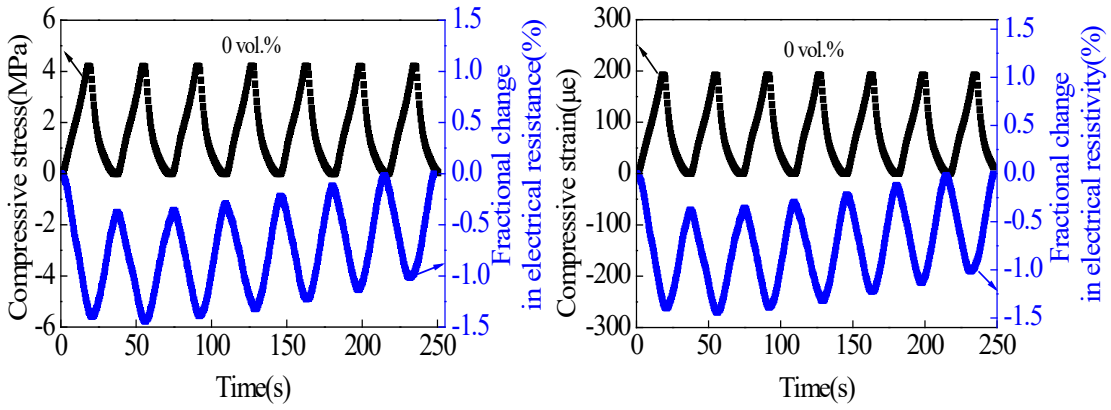

(a) Stress and fractional change in resistivity of S0

(b) Strain and fractional change in resistivity of S0

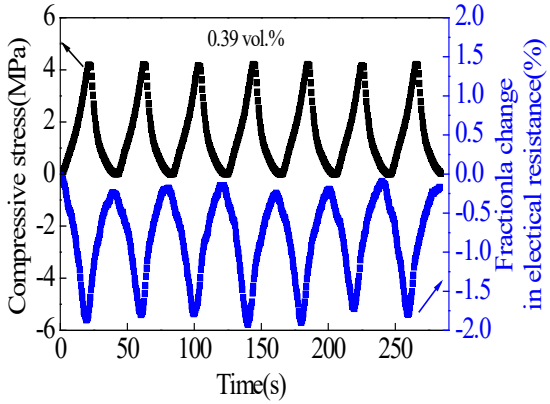

(c) Stress and fractional change in resistivity of S1

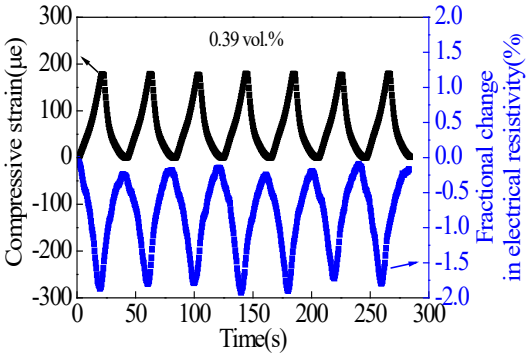

(d) Strain and fractional change in resistivity of S1

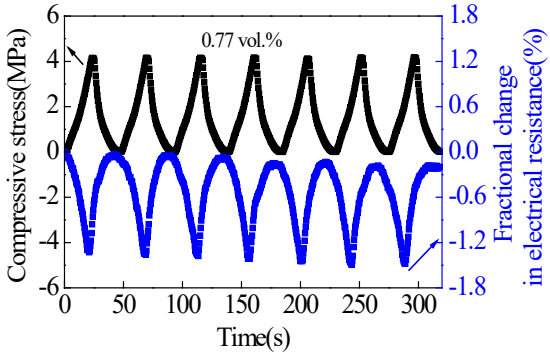

(e) Stress and fractional change in resistivity of S2

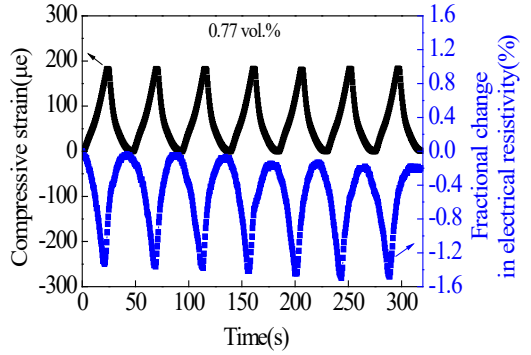

(f) Strain and fractional change in resistivity of S2

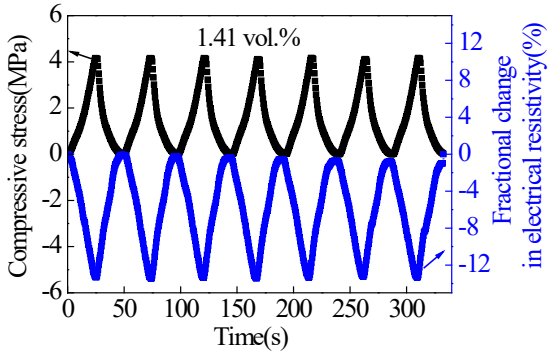

(g) Stress and fractional change in resistivity of S3

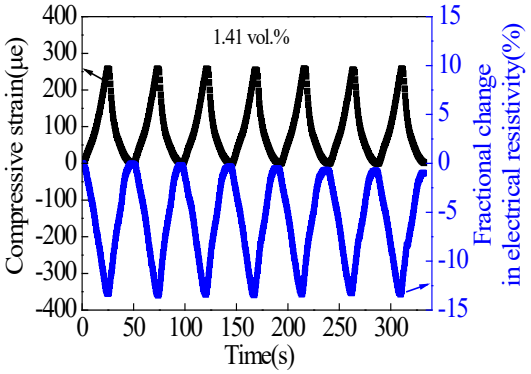

(h) Strain and fractional change in resistivity of S3

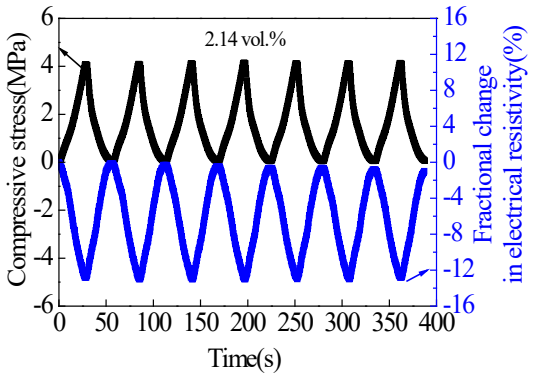

(i) Stress and fractional change in resistivity of S4

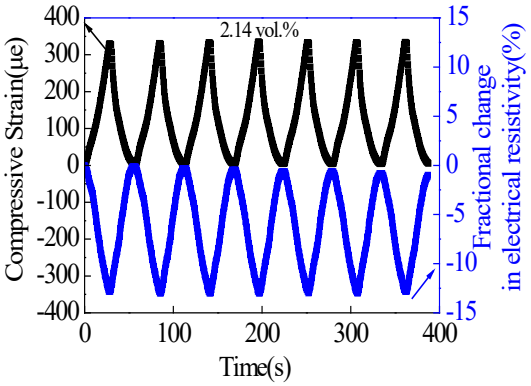

(j) Strain and fractional change in resistivity of S4

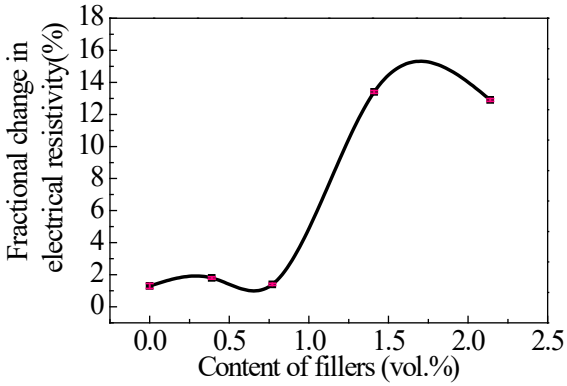

(k) Maximum fraction change in electrical resistivity of S0-S4

Fig. 15 Compressive stress/strain and fractional change in electrical resistivity of S0-S4 under cyclic compressive loading with stress amplitude of 4 MPa after curing in water 28d

Stress and strain sensitivity of S0-S4 under cyclic compressive loading with stress amplitude of 4 MPa after curing in water 28d is shown in Fig. 16. Stress and strain sensitivities both increase and then slightly decrease with increasing content of CNT/NCB composite fillers. The best performance specimen is S3, whose stress and strain sensitivity can reach 3.21%/MPa and 521, respectively.

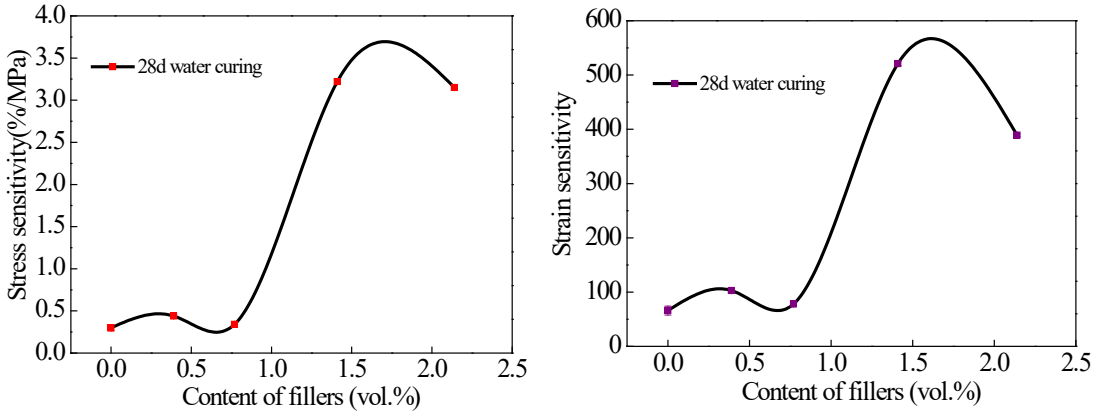

(a) Stress sensitivity (b) Strain sensitivity

Fig. 16 Stress and strain sensitivity of S0-S4 under cyclic compressive loading with stress amplitude of 4 MPa after 28d water curing

Comparison about sensitivity of different piezoresistive cement-based materials with CNT or/and NCB is shown in Table 6. It can be seen that cement-based materials with CNT/NCB composite fillers have the highest stress and strain sensitivity compared with cement-based materials with single CNT or NCB. This is because there are more

distance changes including distance changes between CNT and CNT, NCB and NCB, CNT and NCB. More distance changes mean more conductive network changes in piezoresistive tests then the specimens show high sensitivity. Compared with CNT/NCB fillers owning CNT with large dimeter and small length, cement-based materials with CNT/NCB in this paper have higher stress sensitivity at lower content fillers.

Table 6 Comparison about sensitivity of different piezoresistive cement-based materials with CNT or/and NCB

Filler types	Filler concentration	Stress sensitivity /%MPa^{-1}	Strain sensitivity	Sources
CNT/NCB composite fillers	1.41 vol. %	3.12	521	This paper
	2.40 vol. %	2.69	704	Reference [44]
CNT	0.50 vol. %	0.4	54	Reference [18]
	0.10 vol. %	1.35	-	Reference [26]
	2.00 wt.%	-	220	Reference [27]
NCB	-	1.2	200	Reference [20]
	8.79 vol. %	0.6	60	Reference [25]

(2) Effect of load amplitude on piezoresistive property

The piezoresistive property of cement-based materials with CNT/NCB composite fillers under different load amplitude is shown in Fig. 17. It can be seen from Fig. 17 that all specimens synchronously change with compressive stress/strain levels under different load amplitude. In addition, maximum fractional change in electrical resistivity of all specimens increases with increasing load amplitude. When load amplitude is 2MPa, maximum fractional change in electrical resistivity of S0-S4 is 0.74%, 1.01%, 0.55%, 7.19% and 7.84%, respectively. When load amplitude is 4MPa, maximum fractional change in electrical resistivity of S0-S4 is 1.09%, 1.87%, 1.51%, 12.67% and 11.89%, respectively. Higher load amplitude will lead to increasing more conductive networks. Therefore, maximum fractional change in electrical resistivity increases with increasing load amplitude.

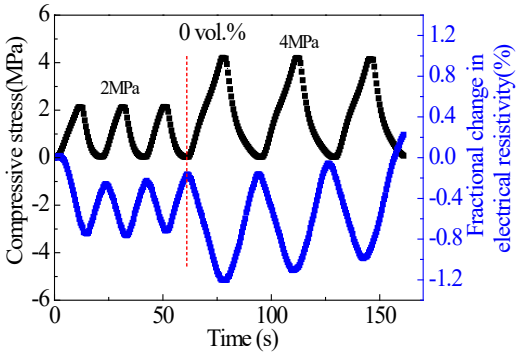

(a) Stress and fractional change in resistivity of S0

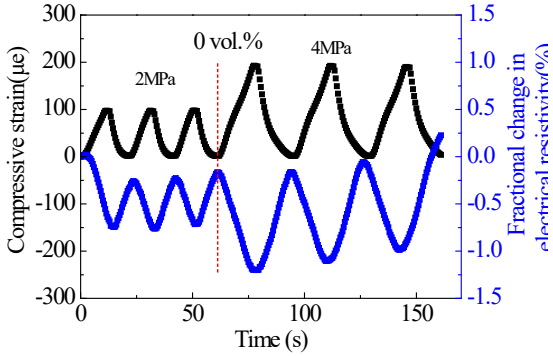

(b) Strain and fractional change in resistivity of S0

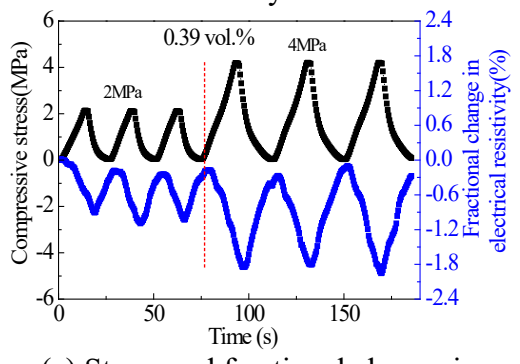

(c) Stress and fractional change in resistivity of S1

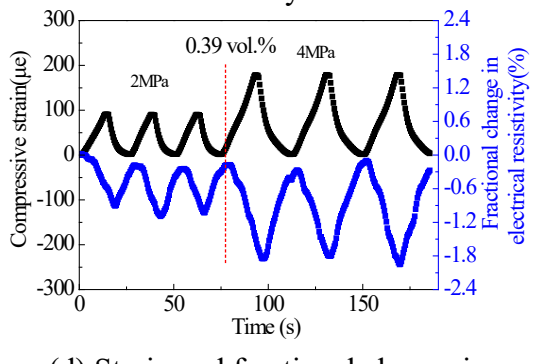

(d) Strain and fractional change in resistivity of S1

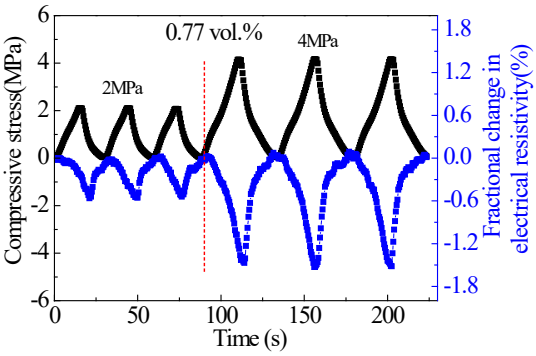

(e) Stress and fractional change in resistivity of S2

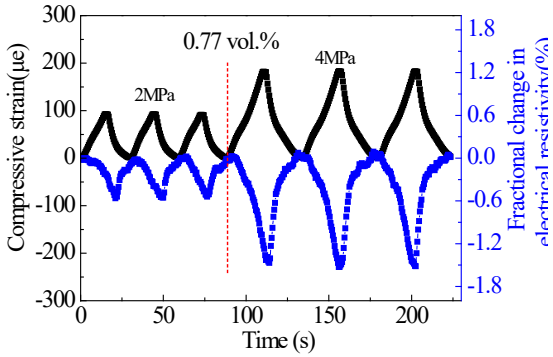

(f) Strain and fractional change in resistivity of S2

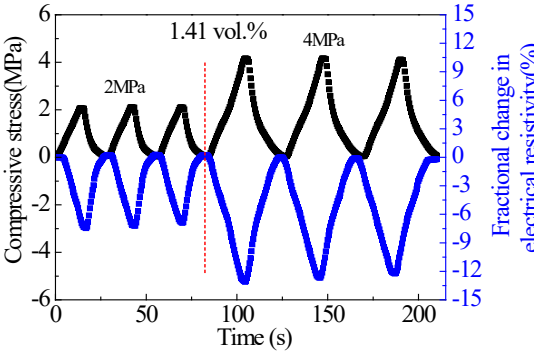

(g) Stress and fractional change in resistivity of S3

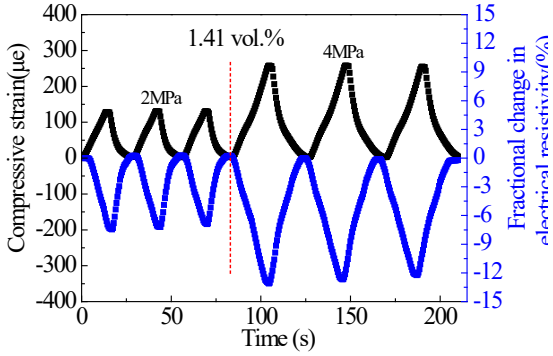

(h) Strain and fractional change in resistivity of S3

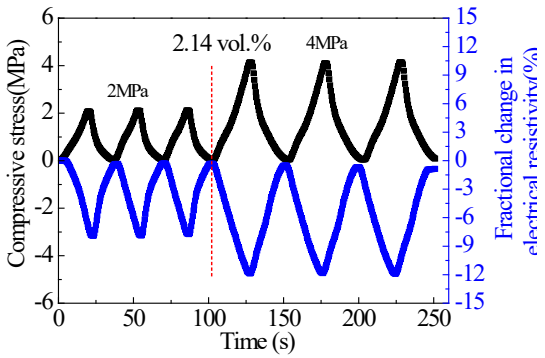

(i) Stress and fractional change in resistivity of S4

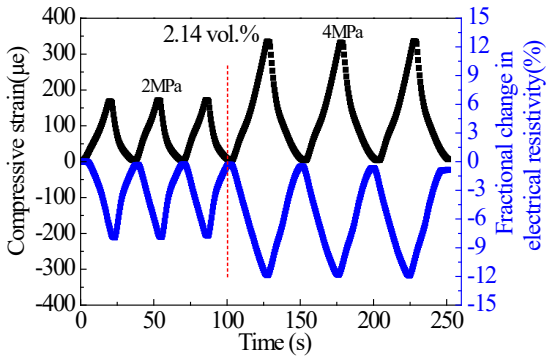

(j) Strain and fractional change in resistivity of S4

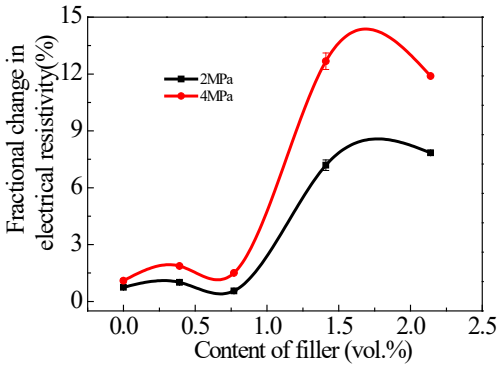

(k) Maximum fraction change in electrical resistivity of S0-S4

Fig. 17 Compressive stress/strain and fractional change in electrical resistivity of S0-S4 under cyclic compressive loading with stress amplitude of 2 MPa and 4 MPa after 28d water curing

Stress and strain sensitivity of S0-S1 under repeated compressive loading with stress amplitude of 2 MPa and 4 MPa after 28d water curing are shown in Fig. 18. When the content of CNT/NCB composite fillers is lower than 1.41 vol. %, the stress and strain sensitivity of the specimens are close under different loading amplitude. The stress sensitivity of cement mortar with 1.41 vol. % CNT/NCB composite fillers under amplitude of 2 and 4MPa is 3.43%/MPa and 3.06%/MPa, respectively. The strain sensitivity of cement mortar with 1.41 vol. % CNT/NCB composite fillers under amplitude of 2 and 4MPa is 554 and 493, respectively. As for cement mortar with 2.14 vol. % CNT/NCB composite fillers, the strain sensitivity under amplitude of 2 MPa and 4 MPa is 3.74%/MPa and 2.88%/MPa, respectively. The strain sensitivity of cement

mortar with 2.14 vol. % CNT/NCB composite fillers under amplitude of 2 MPa and 4 MPa is 462 and 356, respectively.

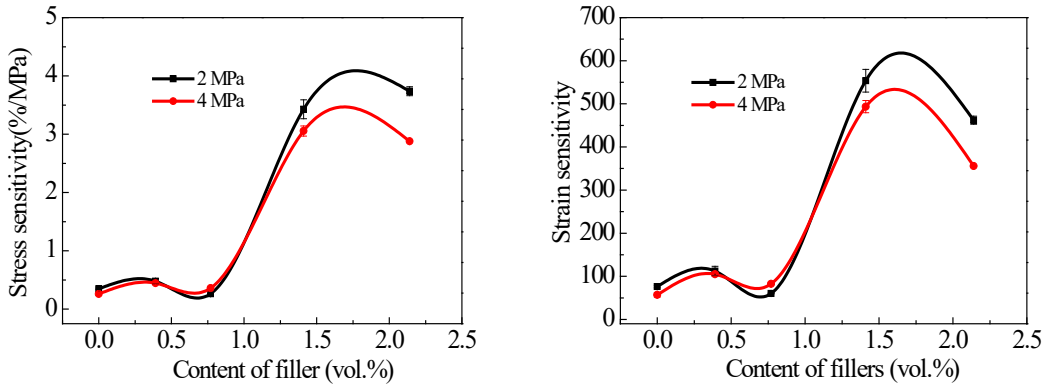

(a) Stress sensitivity (b) Strain sensitivity

Fig. 18 Stress and strain sensitivity of S0-S4 under cyclic compressive loading with stress amplitude of 2 MPa and 4 MPa after 28d water curing

(3) Effect of load rate on piezoresistive property

Compressive stress/strain and fractional change in electrical resistivity of S0-S4 under cyclic loading at loading rate of 0.2, 0.4 and 0.8 mm/min is shown in Fig. 19. At different loading rate, S0-S4 have synchronously change with compressive stress/strain levels under cyclic loading. Fractional change in electrical resistivity of S0 has an increase trend due to the polarization. In addition, the fraction change in electrical resistivity of specimens decreases with increasing load rate.

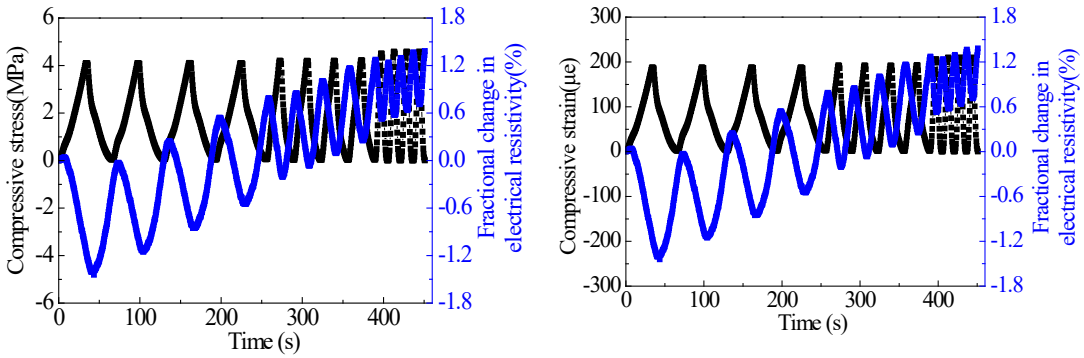

(a) Stress and fractional change in resistivity of S0

(b) Strain and fractional change in resistivity of S0

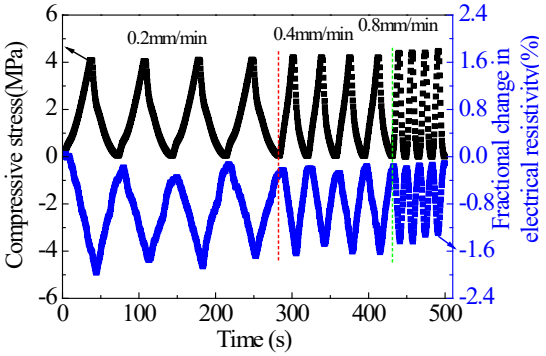

(c) Stress and fractional change in resistivity of S1

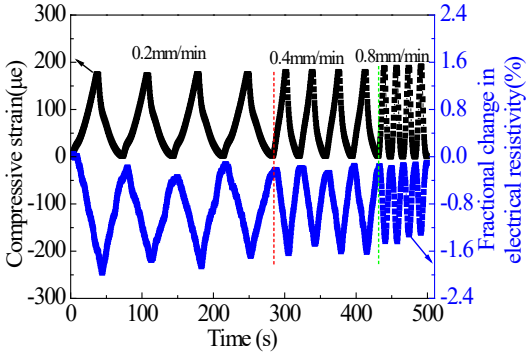

(d) Strain and fractional change in resistivity of S1

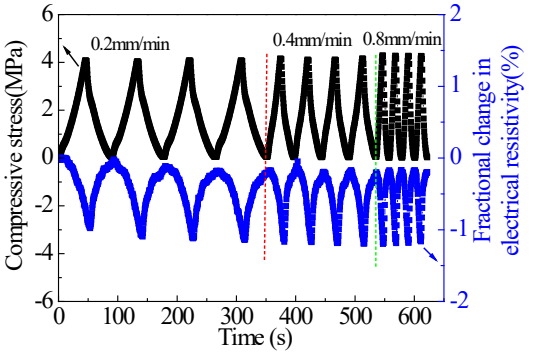

(e) Stress and fractional change in resistivity of S2

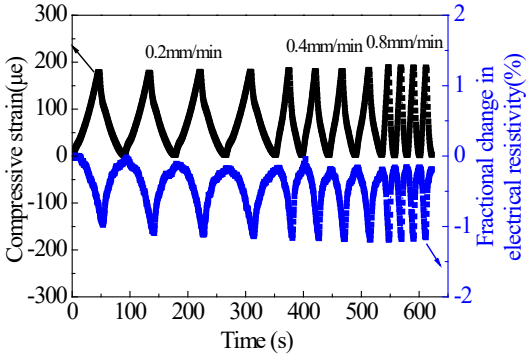

(f) Strain and fractional change in resistivity of S2

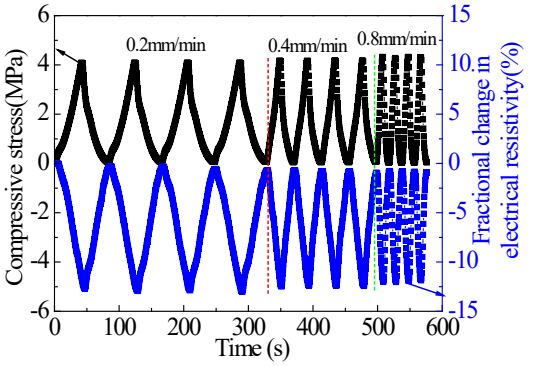

(g) Stress and fractional change in resistivity of S3

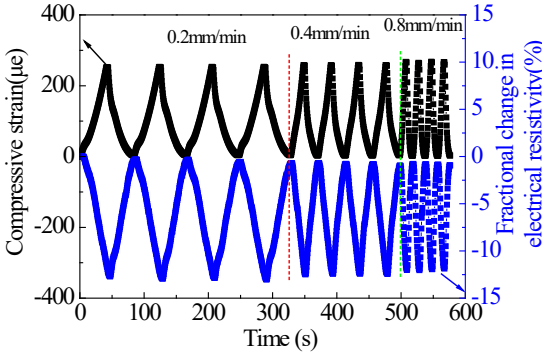

(h) Strain and fractional change in resistivity of S3

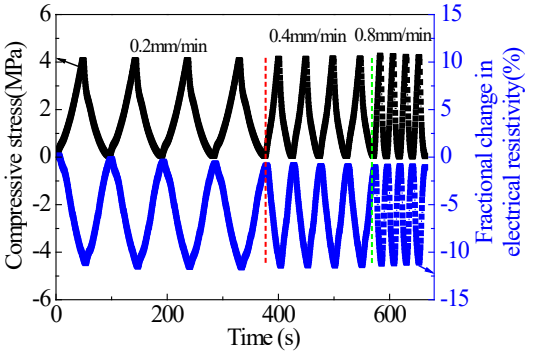

(i) Stress and fractional change in resistivity of S4

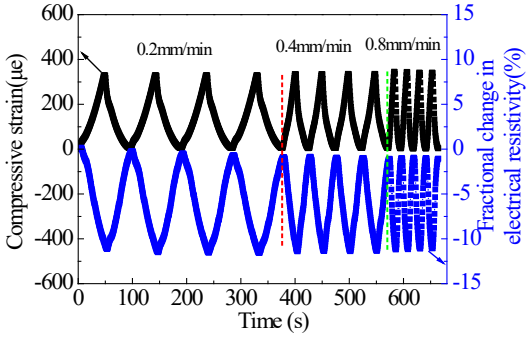

(j) Strain and fractional change in resistivity of S4

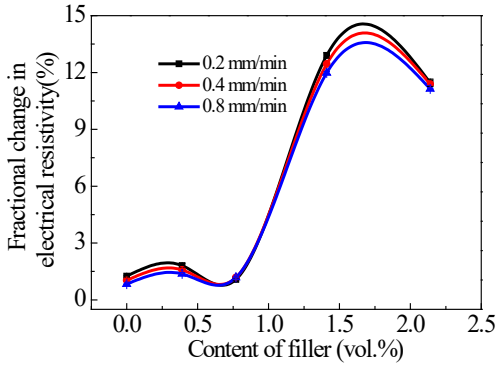

(k) Maximum fraction change in electrical resistivity of S0-S4

Fig. 19 Compressive stress/strain and fractional change in electrical resistivity of S0-S4 at loading rate of 0.2, 0.4 and 0.8 mm/min

Stress and strain sensitivity of S0-S4 at loading rate of 0.2, 0.4 and 0.8 mm/min is shown in Fig. 20. As shown in Fig. 20, stress and strain sensitivity of all specimens decreases with increasing loading rate. It indicates that piezoresistivity of cement-based materials with CNT/NCB composite fillers has a relationship with loading rate [37]. The numbers of pull-in and push-out fillers may decrease due to the increasing loading rate, which is analogous to a smaller amount of cracks formed at the same stress amplitude as the loading rate is higher. This may lead to sensitivity of specimens decreases with increasing loading rate.

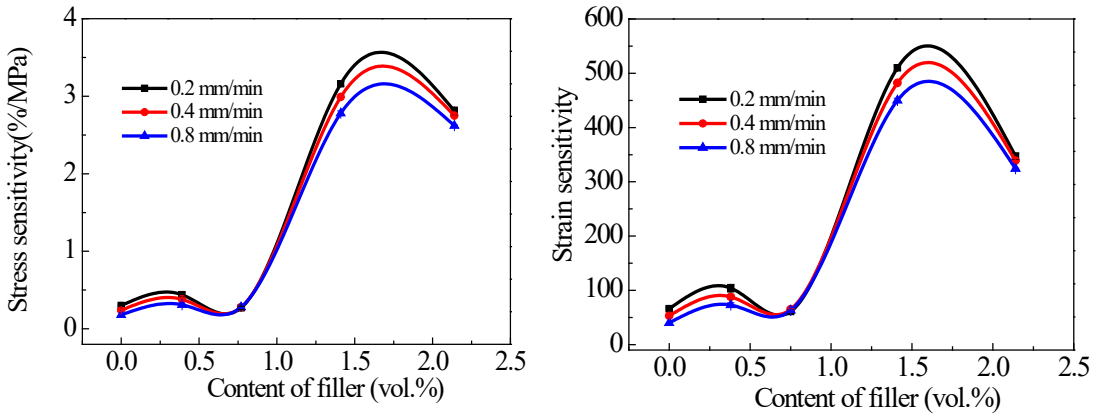

(a) Stress sensitivity (b) Strain sensitivity

Fig. 20 Stress and strain sensitivity of S0-S4 at loading rate of 0.2, 0.4 and 0.8 mm/min

3.3.2 Piezoresistive property under ultimate load

Piezoresitive property of S0-S4 under ultimate load is shown in Fig. 21. As shown in Fig. 21, fractional change in electrical resistivity of all specimens increases with increasing compressive stress or strain. Maximum fractional change in electrical resistivity, stress and strain sensitivity of S0-S4 firstly increases and then decreases with increasing content of CNT/NCB composite fillers. When the content of CNT/NCB composite fillers is 0.77 vol. %, the fractional change in electrical resistivity is 44.6%. The maximum stress and strain sensitivity is 1.29 MPa/% and 208, respectively, when the content of CNT/NCB composite fillers is 1.41 vol. %. The test results indicated that the cement-based materials with CNT/NCB composite fillers can be used to monitor the structural in its whole life.

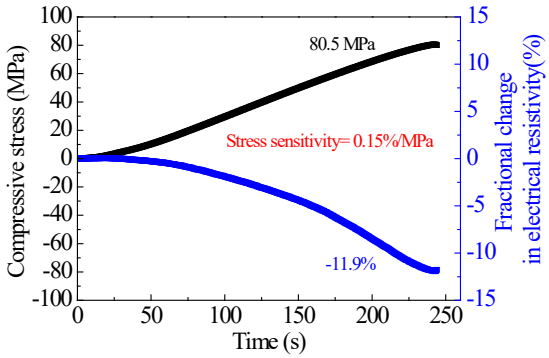

(a) Stress and fractional change in resistivity of S0

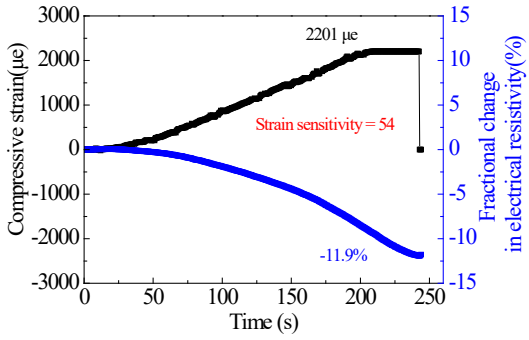

(b) Strain and fractional change in resistivity of S0

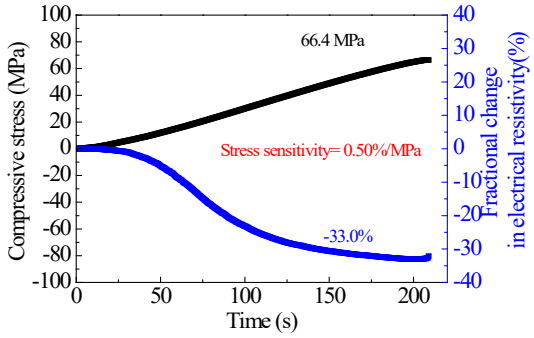

(c) Stress and fractional change in resistivity of S1

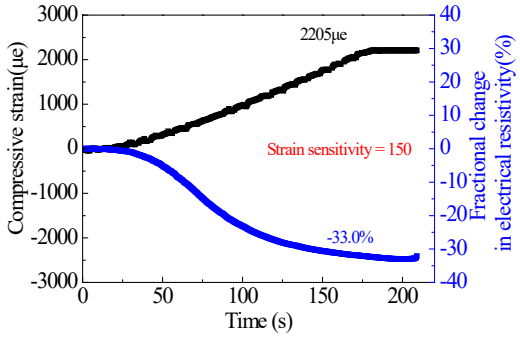

(d) Strain and fractional change in resistivity of S1

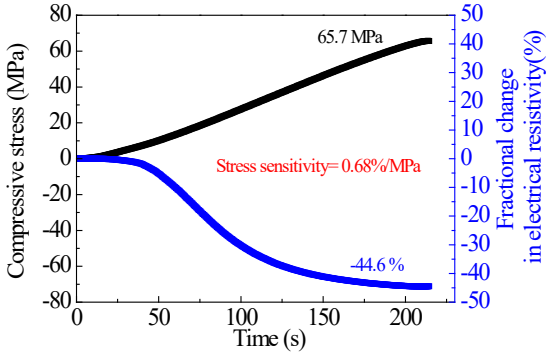

(e) Stress and fractional change in resistivity of S2

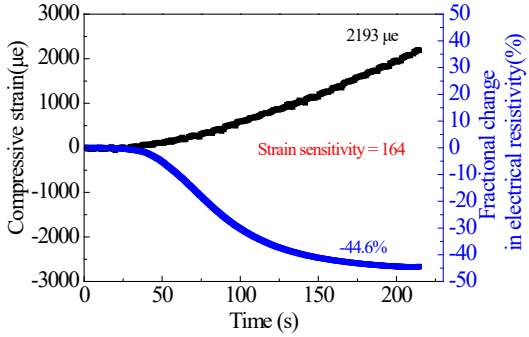

(f) Strain and fractional change in resistivity of S2

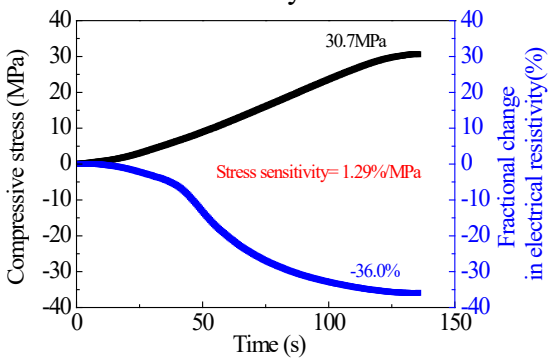

(g) Stress and fractional change in resistivity of S3

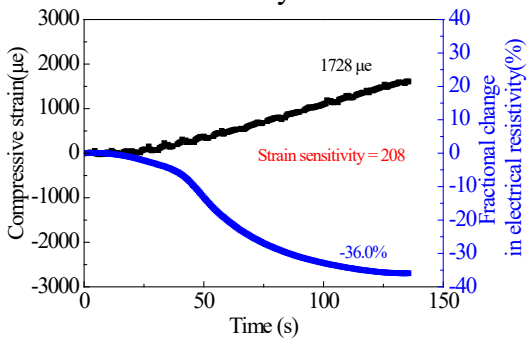

(h) Strain and fractional change in resistivity of S3

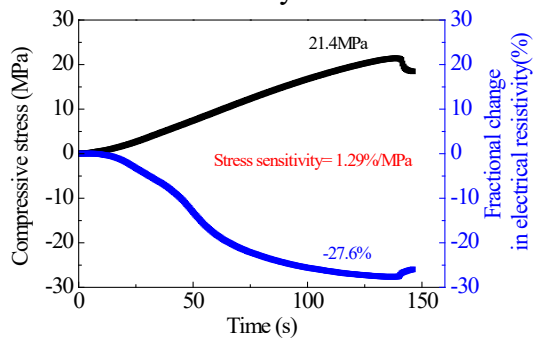

(i) Stress and fractional change in resistivity of S4

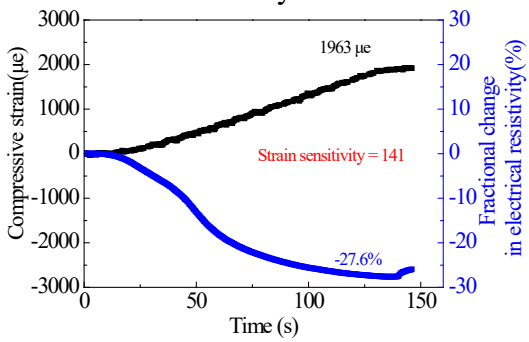

(j) Strain and fractional change in resistivity of S4

Fig. 21 Compressive stress/strain and fractional change in electrical resistivity of S0-S4 under ultimate load

4 Conclusions

Electrostatic self-assembled CNT/NCB composite fillers containing CNT with high aspect ratio and NCB with large size were used to fabricate smart cement-based materials. The flexural and compressive strengths, electrical and piezoresistive property of cement-based materials with CNT/NCB composite fillers were investigated. Conclusions obtained are listed as follows:

(1) Cement-based materials with CNT/NCB composite fillers containing CNT with high aspect ratio and NCB with large size have acceptable mechanical property, low percolation threshold value and high stress sensitivity. Addition of high content of CNT/NCB composite fillers and high water to binder ratios harm the flexural and compressive strength. However, the flexural and compressive strength of cement-based materials with 1.41 vol. % CNT/NCB composite fillers can also reach 7.7 MPa and 30.7 MPa, respectively.

(2) DC electrical resistivity and AC electrical resistivity of cement-based materials both decrease with increasing content of CNT/NCB composite fillers but increase with curing age. The percolation threshold zone is located in the position where the content of CNT/NCB composite fillers is between 0.39 vol. % and 1.41 vol. % from DC electrical resistivity test and AC electrical resistivity test. Percolation equation fits well with DC and AC electrical conductivity. Topological structures of EIS of cement-based materials with various contents of CNT/NCB composite fillers first change before 0.77 vol. % and then keep similar. The chi-squared between measured results and calculated results is less than or equal to 4.05×10^{-4}. Therefore, the selected equivalent circuits are suitable for the cement-based materials with different content of CNT/NCB composite fillers. The calculated values of Rs indicated that CNT/NCB composite fillers increased the porosity of the cement-based materials with CNT/NCB composite fillers.

(3) In elastic regime, fractional change in electrical resistivity, stress and strain sensitivity all firstly increases then decreases with increasing content of CNT/NCB composite fillers. Cement-based materials with 1.41 vol. % CNT/NCB composite fillers has maximum fractional change in electrical resistivity, stress and strain sensitivity, which are 13.4%, 3.21%/MPa, 521, respectively. Maximum fractional change in electrical resistivity of all specimens increase with increasing loading

amplitude, while stress and strain sensitivity of all specimens decrease with increasing loading amplitude. When loading rate increases form 0.2 mm/min to 0.8 mm/min, the fraction electrical resistivity, stress and strain sensitivity of all specimens decrease.

(4) Under ultimate load, maximum fractional change in electrical resistivity, stress and strain sensitivity of S0-S4 firstly increase and then decrease with increasing content of CNT/NCB composite fillers. When the content of CNT/NCB composite fillers is 0.77 vol. %, the maximum fractional change in electrical resistivity is 44.6%. The maximum stress and strain sensitivity is 1.29 MPa/% and 208, respectively, when the content of CNT/NCB composite fillers is 1.41 vol. %.

Acknowledgments

The authors thank the funding supported from the National Science Foundation of China (51578110 and 51428801), and National Key Research and Development Program of China (2017YFC0703410).

References

[1] Han B, Zhang L, Ou J. Smart and Multifunctional Concrete Toward Sustainable Infrastructures. Berlin: Springer, 2017.

[2] Han B, Wang Y, Dong S, Zhang L, Ding S, Yu X, et al.. Smart concrete and structures: a review. J Intel Mater Syst Struct 2015; 26(11): 1303-1345.

[3] Kesavan K, Ravisankar K, Parivallal S, Sreeshylam P, Sridhar S. Experimental studies on fiber optic sensors embedded in concrete. Measurement 2010; 43(2): 157-163.

[4] Leung CKY, Wan KT, Inaudi D, Bao X, Habel W, Zhou Z, et al.. Review: optical fiber sensors for civil engineering applications. Mater Struct 2015; 48(4): 871-906.

[5] Janke L, Czaderski C, Motavalli M, Ruth J. Applications of shape memory alloys in civil engineering structures-Overview, limits and new ideas. Mater Struct 2005; 38(5): 578-592.

[6] Han B, Yu X, Ou J. Self-Sensing Concrete in Smart Structures. Amsterdam: Elsevier, 2014.

[7] Song G, Mo YL, Otero K, Gu H. Health monitoring and rehabilitation of a concrete structure using

intelligent materials. Smart Mater Struct 2006; 15(2): 309.

[8] Tseng KK, Wang L. Smart piezoelectric transducers for in situ health monitoring of concrete. Smart Mater Struct 2004; 13(5): 1017.

[9] Furukawa T, Ishida K, Fukada E. Piezoelectric properties in the composite systems of polymers and PZT ceramics. J Appl Phys 1979; 50(7) 4904-4912.

[10] Chen P, Chung DD L. Concrete as a new strain/stress sensor. Composites Part B: Eng 1996; 27(1) 11-23.

[11] Han B, Ding S, Yu X. Intrinsic self-sensing concrete and structures: A review. Measurement 2015; 59: 110-128.

[12] Saafi M. Wireless and embedded carbon nanotube networks for damage detection in concrete structures. Nanotechnology 2009; 20(39) 844-847.

[13] Luo J. Fabrication and functional properties of multi-walled carbon nanotube/cement composites. Dissertation for the Doctoral Degree in Engineering. Harbin Institute of Technology, Harbin, China. 2009.

[14] Han B, Zhang L, Zeng S, Dong S, Yu X, Yang R, et al.. Nano-core effect in nano-engineered cementitious composites. Compos Part A: Appl Sci Manuf 2017; 95: 100-109.

[15] Shi Z, Chung DDL. Carbon fiber-reinforced concrete for traffic monitoring and weighing in motion. Cem Concr Res 1999; 29(3): 435-439.

[16] Chen P, Chung DDL. Carbon fiber reinforced concrete for smart structures capable of non-destructive flaw detection. Smart Mater Struct 1998; 2(1): 22-30.

[17] Mao Q, Zhao B, Shen D, Li Z. Resistance changement of compression sensible cement specimen under different stresses. J Wuhan Uni of Technol 1996; 11(3): 41-45.

[18] Sun M, Li Z, Mao Q, Shen D. A study on thermal self-monitoring of carbon fiber reinforced concrete. Cem Concr Res 1999; 29(5): 769-771.

[19] Reza F, Yamamuro JA, Batson GB. Electrical resistance change in compact tension specimens of carbon fiber cement composites. Cem Concr Compos 2004; 26(7): 873-881.

[20] Han B, Ou J. Embedded piezoresistive cement-based stress/strain sensor. Sensors Actuat A Phys 2007; 138(2): 294-298.

[21] Han B, Yu Y, Han B, Ou J. Development of a wireless stress/strain measurement system integrated with pressure-sensitive nickel powder-filled cement-based sensors. Sensors Actuat A Phys 2008;

147(2): 536-543.

[22] Han B, Wang Y, Sun S, Yu X, Ou J. Nanotip-induced ultrahigh pressure-sensitive composites: Principles, properties and applications. Compos Part A: Appl Sci Manuf 2014; 59: 105-114.

[23] Han B, Yu X, Kwon E. A self-sensing carbon nanotube/cement composite for traffic monitoring. Nanotechnology 2009; 20: 445501(5pp).

[24] Long X, Sun M, Li Z, Song X. Piezoresistive effects in carbon black-filledcement-matrix nanocomposites. J Wuhan Univ Technol 2008; 30: 57-59.

[25] Li H, Xiao H, Ou J. Effect of compressive strain on electrical resistivity of carbon black-filled cement-based composites. Cem Concr Compos 2006; 28(9): 824-828

[26] Yu X, Kwon E. A carbon nanotube/cement composite with piezoresistive properties. Smart Mater Struct 2009; 18(5): 55010.

[27] Materazzi AL, Ubertini F, Alessandro AD. Carbon nanotube cement-based transducers for dynamic sensing of strain. Cem Concr Compos 2013; 37: 2-11.

[28] Ubertini F, Materazzi AL, Alessandro AD, Laflamme S. Natural frequencies identification of a reinforced concrete beam using carbon nanotube cement-based sensors. Eng Struct 2014; 60: 265-275.

[29] You I, Yoo DY, Kim S, Kim MJ, Zi G. Electrical and Self-Sensing Properties of Ultra-High-Performance Fiber-Reinforced Concrete with Carbon Nanotubes. Sensors 2017; 17(11): 2481.

[30] Sasmal S, Ravivarman N, Sindu BS and Vignesh K. Electrical conductivity and piezo-resistive characteristics of CNT and CNF incorporated cementitious nanocomposites under static and dynamic loading. Compos Part A: Appl Sci Manuf 2017; 100: 227-243.

[31] García-Macías E, D'Alessandro A, Castro-Triguero R, Pérez-Mira D, Ubertini F. Micromechanics modeling of the uniaxial strain-sensing property of carbon nanotube cement-matrix composites for SHM applications. Compos Struct 2017; 163: 195-215.

[32] Han B, Guan X, Ou J. Electrode design, measuring method and data acquisition system of carbon fiber cement paste piezoresistive sensors. Sensors Actuat A Phys 2007; 138(2): 294-298.

[33] Chen B, Liu J. Damage in carbon fiber-reinforced concrete, monitored by both electrical resistance measurement and acoustic emission analysis. Constr Build Mater 2008; 22(11): 2196-2201.

[34] Meehan DG, Wang S, Chung DDL. Electrical-resistance-based sensing of impact damage in carbon fiber reinforced cement-based materials. J Intel Mat Syst Str 2010; 21(1): 83-105.

[35] Chacko RM, Banthia N, Mufti AA. Carbon fiber reinforced cement-based sensors. Can J Civil Eng 2007; 34(3): 284-290.

[36] Wang W, Wu S, Dai H. Fatigue behavior and life prediction of carbon fiber reinforced concrete under cyclic flexural loading. Mater Sci Eng A 2006; 434(1): 347-351.

[37] Dong S, Han B,. Ou J, Li Z, Han L, Yu X. Electrically conductive behaviors and mechanisms of short-cut super-fine stainless wire reinforced reactive powder concrete. Cem Concr Compos 2016;72:48-65.

[38] Sun S, Han B, Jiang S, Yu X, Wang Y, Li H, et al.. Nano graphite platelets-enabled piezoresistive cementitious composites for structural health monitoring. Constr Build Mater 2017; 136: 314-328.

[39] Howser RN, Dhonde HB, Mo YL. Self-sensing of carbon nanofiber concrete columns subjected to reversed cyclic loading. Smart Mater Struct 2011; 20(8): 298-300.

[40] Erdem S, Hanbay S, Blankson MA. Self-sensing damage assessment and image-based surface crack quantification of carbon nanofibre reinforced concrete. Constr Build Mater 2017; 134: 520-529.

[41]

[42] Monteiro AO, Cachim PB, Costa PMFJ. Self-sensing piezoresistive cement composite loaded with carbon black particles. Cem Concr Compos 2017; 81: 59-65.

[43] Al-Dahawi A, Yıldırım G, Öztürk O, Şahmaran M. Assessment of self-sensing capability of Engineered Cementitious Composites within the elastic and plastic ranges of cyclic flexural loading. Constr Build Mater 2017; 145: 1-10.

[44] Han B, Zhang L, Sun S, Yu X, Dong X, Wu T, et al.. Electrostatic self-assembled carbon nanotube/nano carbon black composite fillers reinforced cement-based materials with multifunctionality. Compos Part A: Appl Sci Manuf 2015; 79: 103-115.

[45] Dai Y, Sun M, Liu C, Li Z. Electromagnetic wave absorbing characteristics of carbon black cement-based composites. Cem Concr Compos 2010; 32(7): 508-513.

[46] Boland CS, Khan U, Ryan G, Barwich S, Charifou R, Harvey A, et al.. Sensitive electromechanical sensors using viscoelastic graphene-polymer nanocomposites. Science 2016; 354(6317) 1257-1260.

[47] Zhang L, Han B, Ouyang J, Yu X, Sun S, Ou J. Multifunctionality of cement based composite with electrostatic self-assembled CNT/NCB composite filler. Arch Civ Mech Eng 2017; 17(2): 354-364.